Lawrence Berkeley National Laboratory
Recent Work

Title
ROD-LIKE DEFECTS IN ION IMPLANTED SILICON

Permalink
https://escholarship.org/uc/item/9c59h8pj

Author
Wu, Wei-Kuo

Publication Date
1976-04-01

eScholarship.org Powered by the California Digital Library
University of California

Submitted to Crystal Lattice Defects

LBL-4192
Preprint C.1

ROD-LIKE DEFECTS IN ION IMPLANTED SILICON

Wei-Kuo Wu and Jack Washburn

RECEIVED
LAWRENCE
BERKELEY LABORATORY

JUL 26 1976

LIBRARY AND
DOCUMENTS SECTION

April 1976

Prepared for the U. S. Energy Research and
Development Administration under Contract W-7405-ENG-48

For Reference

Not to be taken from this room

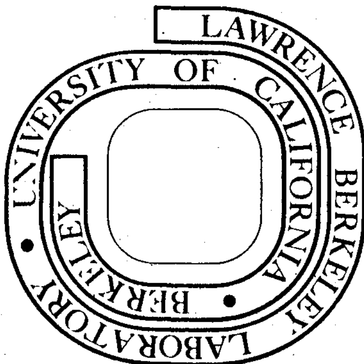

LBL-4192
C.1

DISCLAIMER

This document was prepared as an account of work sponsored by the United States Government. While this document is believed to contain correct information, neither the United States Government nor any agency thereof, nor the Regents of the University of California, nor any of their employees, makes any warranty, express or implied, or assumes any legal responsibility for the accuracy, completeness, or usefulness of any information, apparatus, product, or process disclosed, or represents that its use would not infringe privately owned rights. Reference herein to any specific commercial product, process, or service by its trade name, trademark, manufacturer, or otherwise, does not necessarily constitute or imply its endorsement, recommendation, or favoring by the United States Government or any agency thereof, or the Regents of the University of California. The views and opinions of authors expressed herein do not necessarily state or reflect those of the United States Government or any agency thereof or the Regents of the University of California.

ROD-LIKE DEFECTS IN ION IMPLANTED SILICON

Wei-Kuo Wu* and Jack Washburn

ABSTRACT

Two kinds of rod-shaped defects formed during post-implantation annealing of silicon which has been implanted with boron ions to a dose ($2 \times 10^{14}/cm^2$) have been identified by contrast analysis of transmission electron micrographs.

All rods initially have a long axis along a<110> direction. From the contrast analysis, it has been concluded that one set can best be described as elongated imperfect (Frank) dislocation loops or dipoles on {111} planes with Burgers vector perpendicular to the loop plane. The second type has a habit plane near to {100} and a displacement vector which is probably perpendicular to the habit plane. Both kinds are interstitial in nature.

*Present Address: Hewlett Packard Company, 11000 Wolfe Road, Cupertino, California 95014

00004401302

INTRODUCTION

Long rod-like defects of the type observed in ion implanted silicon were first reported by Mazey, Barnes and Nelson for neon irradiated silicon[1]. Later, they were found in boron[2] and phosphorous[3] implanted silicon. Similar defects were also observed in high energy electron irradiated silicon[4].

The precise nature of these defects is still rather mysterious; they have been described as precipitates, lines of point defects or as elongated loops by the above authors. Most recently, Madden and Davidson[5] studied these defects in boron irradiated silicon. After detailed analysis, in which they excluded all the other possibilities, they concluded that the rods must be elongated faulted dislocation loops, extrinsic in character with an a/k<100> Burgers vector. They also concluded from the existence of rod-like defects after implanting silicon with various different ions that the defects are composed mostly of silicon atoms.

In the present work, specimens from wafers of three different orientations were examined, <111>, <110> and <100> in order to permit identification of Burgers vectors and habit planes with more certainty than in previous investigations.

The small dislocation loops which are also present have been studied extensively in the past[2,6] and will not be considered here. Also excluded from the present discussion are rod defects that do not lie along <110>. These are formed during annealing by transformation of the "{111}" type defects and will be discussed elsewhere.

EXPERIMENTAL

1. Specimen Preparation

N-type silicon slices, 5Ω-cm, of <111> and <100> orientation were irradiated at room temperature with Boron ions at 100kV to a dose of

$2 \times 10^{14}/cm^2$.

Specimens of 3mm in diameter for electron microscope observation were ultrasonically cut from the slices. They were then annealed in a quartz tube furnace with flowing dry nitrogen passing through it. The annealed specimens were then chemically polished from the unimplanted side in one part solution A (2.5gm iodine and 1100ccCH_3COOH) and two parts solution B (1HF + $3HNO_3$). Polishing was stopped when a small hole appeared at the center of the disc.

2. Electron Microscopy

All the specimens were examined in the Philips 301 transmission electron microscope operating at 100 kV. A double tilting stage facilitated high angle tilting up to 60°. All micrographs were taken under two beam diffraction conditions with $S>0$. +g and -g micrographs were used so as to show loops in both inside and outside contrast.

All the micrographs were indexed and analyzed by making use of the Kikuchi map as described previously[7].

RESULTS

1. General Observations

The long rod-like defects appeared after annealing at 700°C. They were observed to lie in all six <110> projected directions, but the ones on the inclined <110> directions were usually shorter than those parallel to the surface for a <111> implanted foil (Fig. 1). No such obvious difference in length was observed for <100> implanted foils.

Although the width of the rod-like defects was small, when the $\vec{g}$ vector was changed from +g to -g, some of them were clearly resolved as loops or dipoles showing inside and outside contrast[8] characteristic

of dislocation loops (Fig. 2). Figure 2 shows that parallel defects often show different diffraction contrast for a given diffraction condition. For example, A shows inside while a shows outside contrast and vice versa. Both these defects went out of contrast completely when the diffracting vector was parallel to the rod direction.

2. Contrast Analysis

a) Determination of Burgers Vectors

In order to determine the Burgers vector unambiguously by contrast analysis, observation of the same defect for many different low index $\vec{g}$ vectors is necessary. <100> oriented foils were used in addition to <111> foils and the selection of different $\vec{g}$ vectors was facilitated by a high angle tilting stage which could be rotated up to 60° in any direction.

A typical example is shown in Fig. 3. Figures 3a through d were taken near [001] orientation. The foil was then rotated to [011] and $[0\bar{1}1]$* orientation with the diffracting $\vec{g}$ vectors as indicated (Fig. 3e and f). It is seen that linear defects a and d are showing very weak contrast in [001] orientation, while A, $\bar{A}$ and D are showing strong inside and outside contrast. When the foil is tilted away from [001] to either $[0\bar{1}1]$ or [011] orientation, a and d also show strong contrast. It is noted that A and $\bar{A}$ show different contrast in Fig. 3a and b. This might be due to the fact that one is interstitial type and one is vacancy type

---

* Micrographs taken near $[0\bar{1}1]$ orientation with [022] diffracting vectors were not included in this figure. However, the observed diffracting contrast is tabulated in Table 1.

00004401204

or that they have different inclinations. The different contrast of A and $\bar{A}$ is also shown in Figs. 3e and f, where defect $\bar{A}$ shows the same strong contrast when the $\vec{g}$ is reversed in direction (typical of a nearly edge-on view) while defect A shows very weak residual contrast [8]. The reverse is observed in $[0\bar{1}1]$ orientation.

A contrast analysis showing contrast observed for different g vectors for each of these linear defects is shown in Table I. For example, only a Burgers vector along the $[\bar{1}\bar{1}\bar{1}]$ direction is consistent with all the observed contrast changes for loop A. Other Burgers vectors such as [001] or $[\bar{1}\bar{1}0]$ can not satisfy the observed contrast either in [011] or $[0\bar{1}1]$ orientation. Similarly, only $[11\bar{1}]$ and $[\bar{1}1\bar{1}]$ satisfies all observed contrast for loops $\bar{A}$ and D respectively.

A very weak contrast for defects a and d in [001] orientation for all different diffracting $\vec{g}$ vectors suggests that the Burgers vector is near to being parallel to the beam direction, e.g., [001]. The contrast observed in [011] and $[0\bar{1}1]$ orientations for defect a and d is also consistent with a Burgers vector near $[00\bar{1}]$.

The existence of linear defects with Burgers vectors near <100> with a habit plane perpendicular to the Burgers vector is also consistent with the contrast observations for the defects along the inclined <110> directions, e.g., b, c, e and f in Fig. 3. These defects all show about the same kind of contrast when the g is reversed in direction (typical of a nearly edge-on view) in Fig. 3a to c. They show very weak contrast or are invisible when the $\vec{g}$ vectors are parallel to the projected rod directions in Fig. 3d. complete contrast observations for these defects are also shown in Table 1.

b) Determination of Habit Planes and Loop Types

The loop plane for loop A, $\bar{A}$ and D was inferred from the orientation where it showed "edge-on behavior". It was concluded that loop A, $\bar{A}$ and D observed in this case were all elongated faulted Frank dislocation loops or dipoles with {111} habit planes and interstitial character.

The habit planes for defects a and d were difficult to determine in this orientation, since a tilting of nearly 90° would probably be required to make them edge-on. However, some defects like a, did show inside and outside contrast in both [0$\bar{1}$1] and [011] orientations as shown in Fig. 4. The similar appearing rods in Fig. 3 are too narrow to be resolved. In a <111> foil, the spacing of defect c, in Fig. 5, was observed to increase as tilted from <111> to<112> orientation (compare the spacing of defect c in Fig. 2 and 3. This makes either {111} or {110} unlikely as its habit plane because for either of these planes there should have been a decrease in the apparent spacing of the defect when tilted from <111> to <112>. The observed behavior is consistent with the idea that rod defects of this kind are lying on or near the {100} planes.

DISCUSSION AND CONCLUSION

From the above results, it was concluded that there are at least two kinds of rod-like defects. They are all interstitial in nature. One kind is on the {111} planes with Burgers vectors a/x<111> perpendicular to the loop plane. The other kind is on or near {100} with Burgers vector approximately a/x<100> perpendicular to the habit plane. The magnitudes of the Burgers vectors are impossible to determine from the contrast analysis due to the narrow spacings of the defects.

0 0 0 0 4 4 0 1 3 0 5

Thin foil annealing experiments to be reported elsewhere suggest that the rod-like defects of "{100}" type contain some boron atoms. The temperature dependence of their shrinkage rate corresponds to that of boron diffusion in silicon. The defects of "{111}" type anneal out with a higher apparent activation energy which is close to that observed for silicon self diffusion in the same temperature range.[9]

The formation of two different kinds of rod-like defects suggests that boron interstitials or a combination of boron and silicon interstitials are precipitated on or nearly on {100} and that silicon interstitials can form elongated Frank loops on {111} planes.

ACKNOWLEDGEMENTS

This work was done under the auspices of the Materials and Molecular Research Division, Lawrence Berkeley Laboratory, of the U. S. Energy Research and Development Administration.

REFERENCES

1. D. J. Mazey, R. S. Barnes and R. S. Nelson, Proc. 6th International Conf. on Electron Microscopy, Kyoto, 363 (1966).
2. R. W. Bicknell, Proc. Royal Soc., 311, 75 (1969).
3. K. Seshan and J. Washburn, Rad. Effects, 14, 267 (1972).
4. E. Nes and J. Washburn, J. Appl. Phys., 42, 3559 (1971).
5. P. K. Madden and S. M. Davidson, Rad. Effects, 14, 271 (1972).
6. W.-K. Wu and J. Washburn, J. Appl. Phys. 45, 1085 (1974).
7. W.-K. Wu, L.-J. Chen, J. Washburn and G. Thomas, J. Appl. Phys., 45, 563 (1974).
8. P. B. Hirsch, A. Howie, R. B. Nicholson and D. W. Pashley, Electron Microscopy of Thin Crystals, (Butterworths, London, 1965).
9. W.-K. Wu, Lawrence Berkeley Laboratory Report No. 3758, to be published.

0 0 0 0 4 4 0 1 3 0 6

TABLE I. Diffraction Contrast of Rod-like Defects With Different g Vectors.

	$\vec{g}$								
	$\hat{n}$ = [001]				$\hat{n}$ = $[0\bar{1}1]$	$\hat{n}$ = [011]			
Defect No.	[220]	$[2\bar{2}0]$	$[\bar{4}00]$	[040]	[022]	$[0\bar{2}2]$	$\vec{b}$	$\vec{n}$	Type
A	O	N	I	O	E-O	R	$[\bar{1}\bar{1}\bar{1}]$	[111]	Interstitial
$\bar{A}$	I	N	O	I	R	E-O	$[11\bar{1}]$	$[\bar{1}\bar{1}1]$	Interstitial
D	N	O	I	I	R	E-O	$[\bar{1}1\bar{1}]$	$[\bar{1}1\bar{1}]$	Interstitial
a	R	N	R	R	O	O	$[00\bar{1}]$	[001]	Interstitial
b	E-O	E-O	E-O	R	H-O	N	±[100]		
c	E-O	E-O	R	E-O	I	I	±[010]	$\pm[0\bar{1}0]$	Interstitial
d	N	R	R	R	O	O	$[00\bar{1}]$	[001]	Interstitial
c	E-O	E-O	R	E-O	I	I	±[010]	$\pm[0\bar{1}0]$	Interstitial
f	E-O	E-O	E-O	R	N	H-O	±[100]		

O Outside Contrast
I Inside Contrast
R Residual Contrast; $\vec{g}.\vec{b} = 0$, $\vec{g}.\vec{b}\times\vec{u} \neq 0$
N No Contrast; $\vec{g}.\vec{b} = 0$, $\vec{g}.\vec{b}\times\vec{u} = 0$
E-O Edge-On
H-O Head-On

FIGURE CAPTIONS

Fig. 1. Typical crystal defects formed after post-implantation annealing in boron ion implanted silicon in a [111] orientation. More than two different $\vec{g}$ vectors were strongly excited, so that all six different sets of rod-like defects along <110> are shown.

Fig. 2. Two different kinds of rod-like defects, A and a parallel to each other, but showing opposite diffracting contrast.

Fig. 3. Diffraction contrast of rod-like defects in different orientations. (a) through (d) are near <001> orientation. (e) and (f) are near <011> orientation.

Fig. 4. Diffraction contrast of rod-like defects as in Fig. 3. Note that defect a shows inside and outside contrast in both $[\bar{1}01]$ and [011] orientation. This excludes the possibility of its being on a {111} habit plane. The tiny spots in the background are due to use of a deoxide etch after the thin foil was made.

Fig. 5. The weak beam dark field diffraction contrast of defects as observed at different orientations. (1) and (2) are near [111] orientation, (3) and (4) are near [211]. Note that the spacing for rod-like defect c increases as tilted from [111] to [211] orientation.

0 0 0 0 4 4 0 1 3 0 7

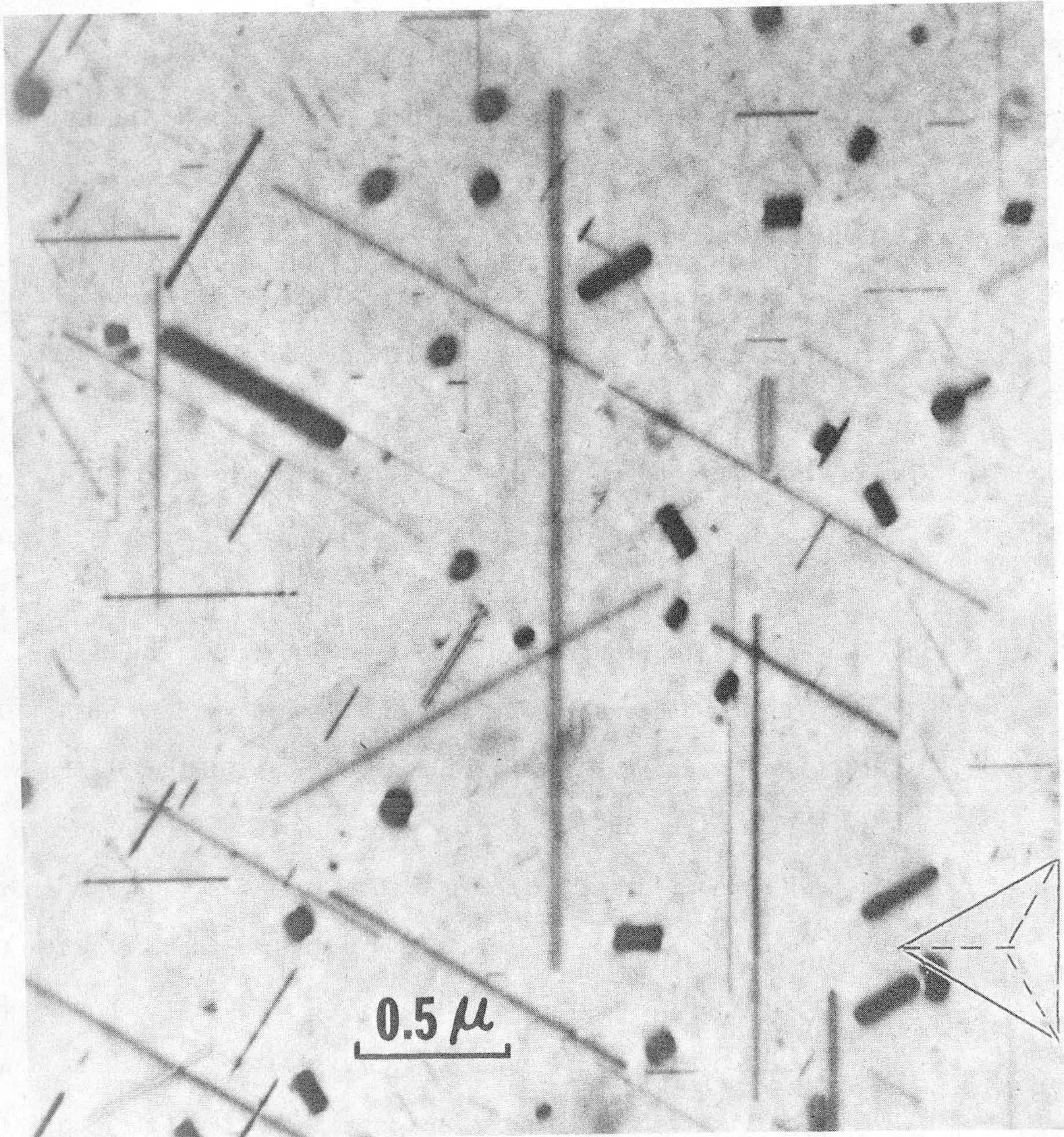

Fig. 1 XBB 763-3113

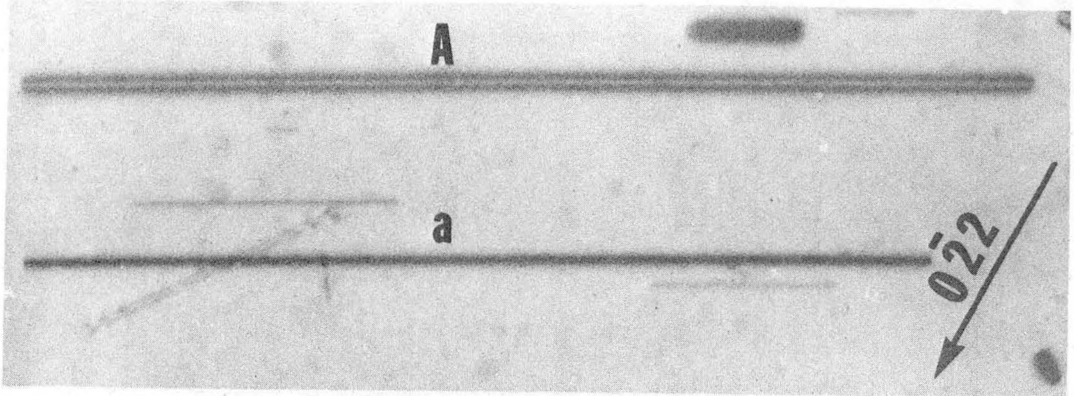

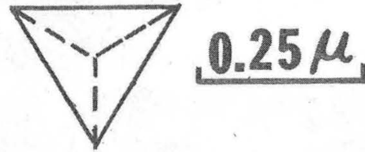

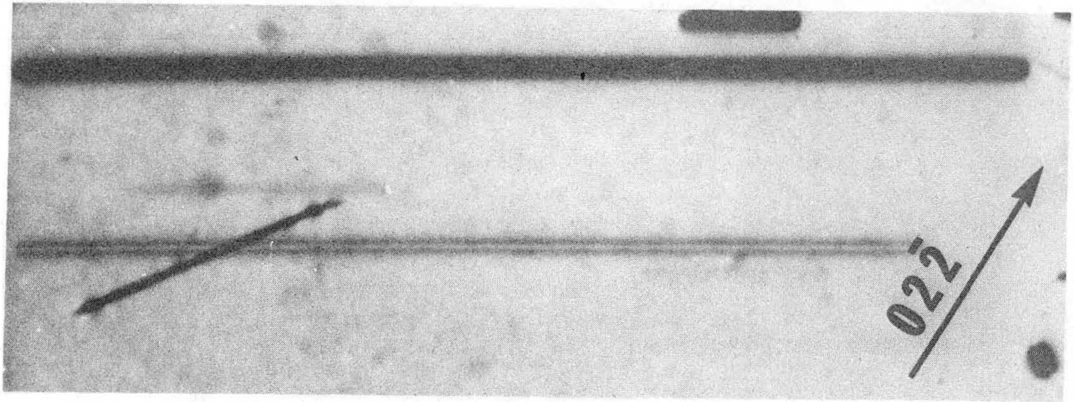

Fig. 2 XBB 763-3111

0 0 0 0 4 4 0 1 3 0 8

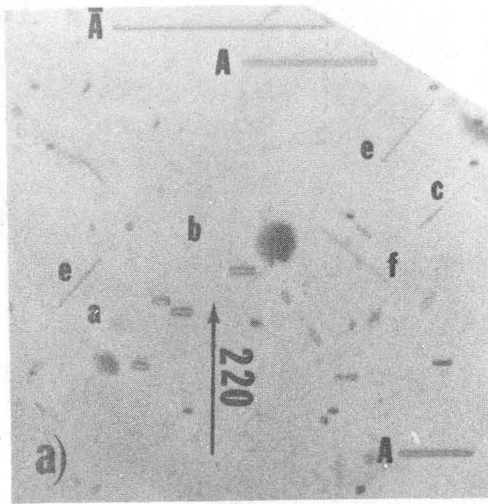

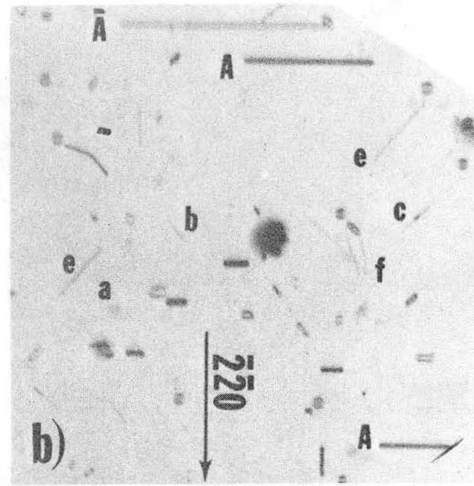

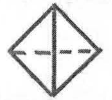

n=[001]

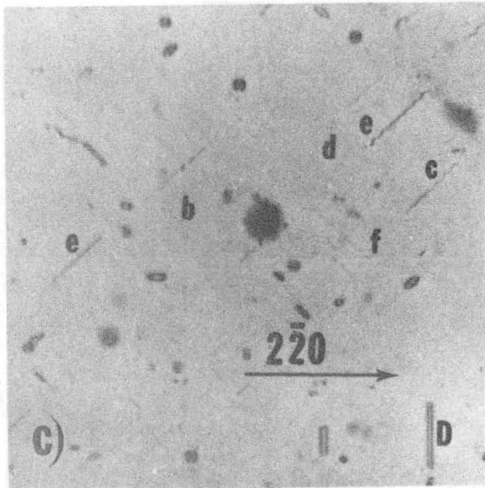

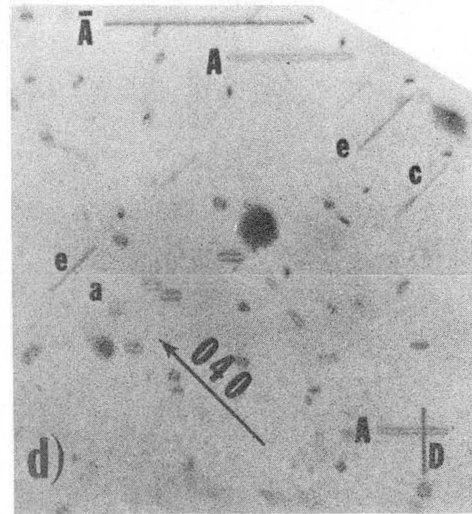

0.5 μ

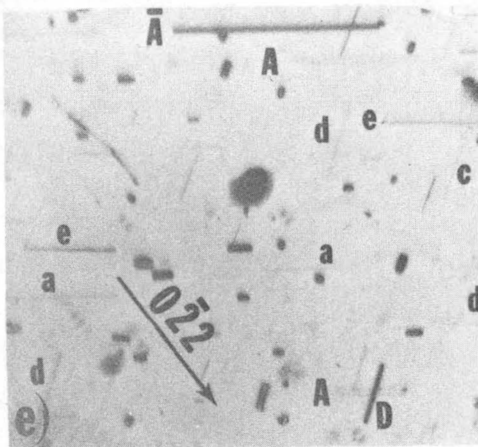

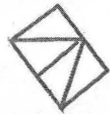

n=[011]

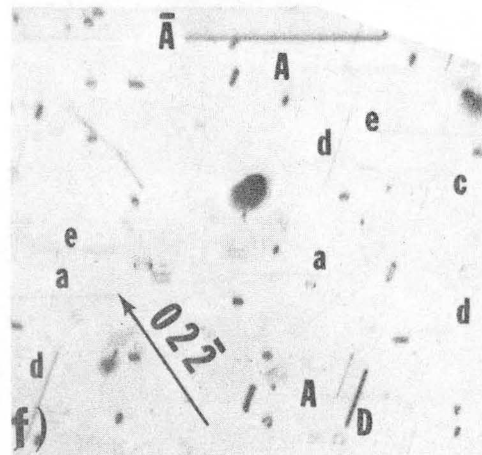

Fig. 3

XBB 763-3109

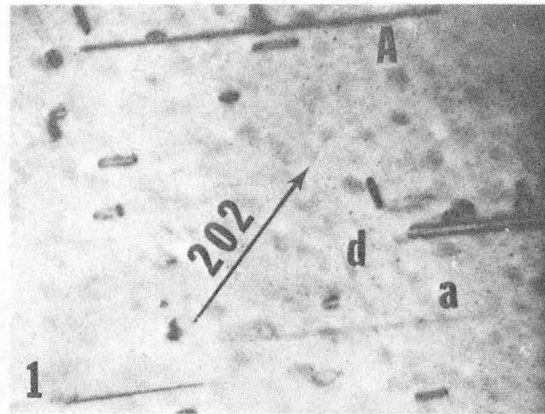

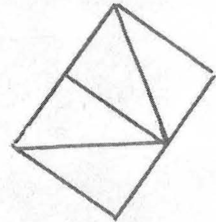

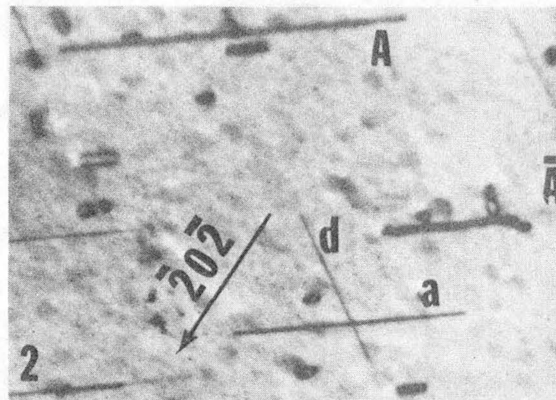

0.5 μ

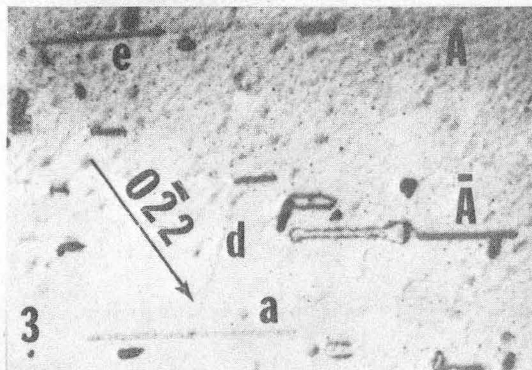

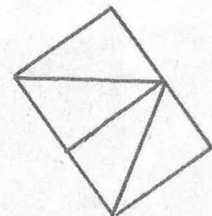

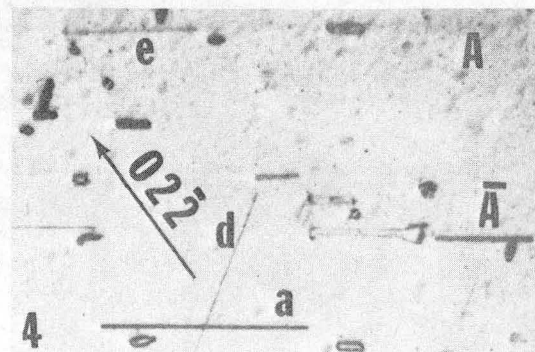

Fig. 4 XBB 763-3110

0 0 0 0 4 4 0 1 2 0 9

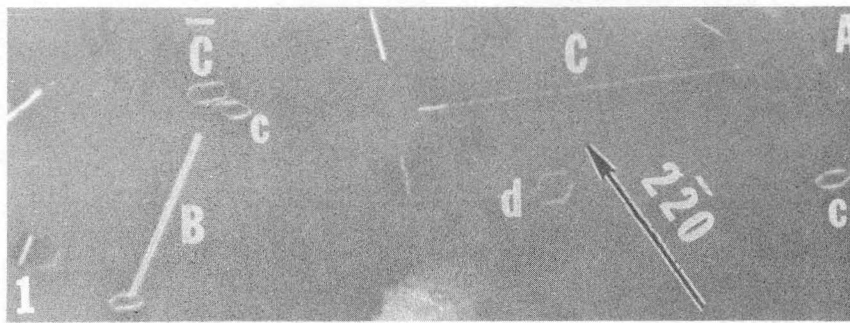

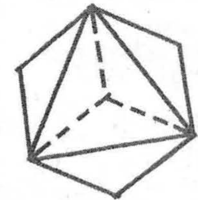

0.5 μ

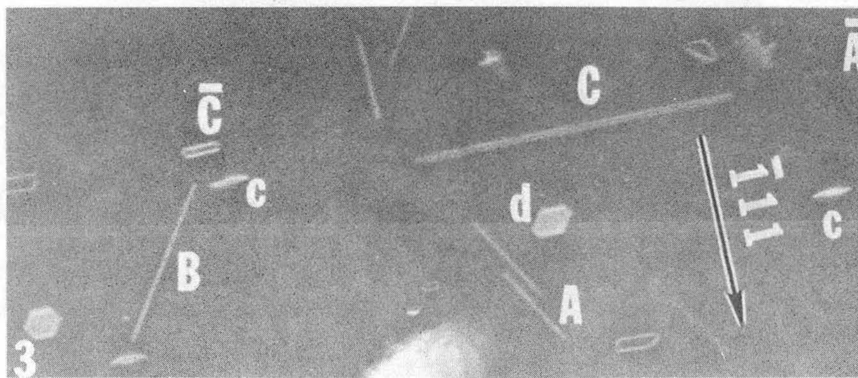

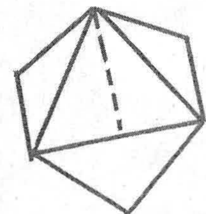

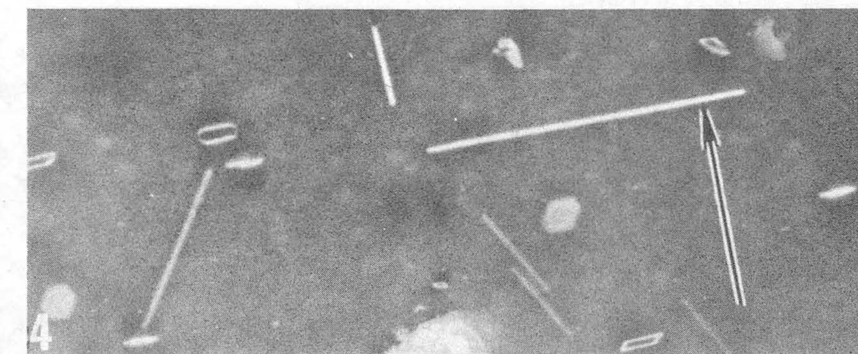

Fig. 5 XBB 763-3112

LEGAL NOTICE

This report was prepared as an account of work sponsored by the United States Government. Neither the United States nor the United States Energy Research and Development Administration, nor any of their employees, nor any of their contractors, subcontractors, or their employees, makes any warranty, express or implied, or assumes any legal liability or responsibility for the accuracy, completeness or usefulness of any information, apparatus, product or process disclosed, or represents that its use would not infringe privately owned rights.

TECHNICAL INFORMATION DIVISION
LAWRENCE BERKELEY LABORATORY
UNIVERSITY OF CALIFORNIA
BERKELEY, CALIFORNIA 94720